

# Optical characteristics of ordinary and tunable 1D Si photonic crystals in the mid-infrared range

Vladimir Tolmachev<sup>a,b</sup>, Tatiana Perova<sup>\*a</sup>, Ekaterina Astrova<sup>b</sup>, Jyulia Pilyugina<sup>b</sup>, Alan Moore<sup>a</sup> and Kevin Berwick<sup>c</sup>

<sup>a</sup> Department of Electronic and Electrical Engineering, University of Dublin, Trinity College, Dublin 2, Ireland; <sup>b</sup> Ioffe Physico-Technical Institute, Polytechnicheskaya 26, St.-Petersburg, Russia;

<sup>c</sup> Department of Electronic and Communications Engineering, Dublin Institute of Technology, Kevin St, Dublin 8, Ireland

## ABSTRACT

Reflection spectra and photonic band gaps (PBGs) for periodic structures consisting of grooved Si infiltrated with nematic liquid crystals (LCs) E7 have been obtained experimentally and by simulation. Periodically grooved Si matrixes, with lattice periods ranging from 2 to 6  $\mu\text{m}$ , were fabricated using wet anisotropic etching of (110) Si in an alkaline solution. It is shown theoretically that a substantial shift of PBGs can be obtained when there is a homogeneous alignment of the liquid crystal molecules with respect to the Si walls and, therefore, a change in the LC's refractive index from  $n_o$  to  $n_e$  during electro-tuning can be expected. This effect is smaller during thermo-tuning effect when refractive index changed from  $n_o$  to,  $n_i$  (isotropic LC phase). The simulated reflection spectra are in good agreement with experimental data obtained with a Digilab FTS 6000 FTIR spectrometer in conjunction with a UMA 500 infrared microscope. A shift of the PBG's edges by a factor  $\Delta\lambda/\lambda=7\%$  was predicted as a result of a thermo-tuning effect and  $\sim 10\%$  as a results of electro-tuning effect.

**Keywords:** 1D photonic crystals, photonic gap map, birefringence, FTIR microscopy, nematic liquid crystals

## 1. INTRODUCTION

Photonic crystals (PCs) are materials with a regular change in the refractive index,  $n$ . The periodicity in the refractive index is of the order of the wavelength of light<sup>1</sup> and can be in one, two or three dimensions. A forbidden gap for photons within a particular frequency range, similar to that for electrons in atomic crystals, arises for structures with appropriate values of refractive index, symmetry and period. This gap is known as a photonic band gap (PBG) and leads to the appearance of stop bands in reflection or transmission spectra. Numerous publications have been devoted to one dimensional (1D) photonic crystals (PCs) over the several decades and they are now widely used as multilayer periodical structures<sup>1,2</sup>. These structures are fabricated by methods based on multilayer coatings or on the fabrication of periodic layers with different porosities on the substrate. Both methods result in structures with vertically aligned layers and, therefore, with a vertical modulation of refractive index,  $n$ , with respect to the substrate.

Recently, a number of new methods of fabricating 1D PCs with a horizontal modulation of  $n$ , so called planar PCs, have been published<sup>3-6</sup>. These new fabrication processes include a standard photolithography step with patterning of windows with a particular shape on the surface of semiconductor material followed by wet or dry etching of the substrate material. Use of a wet etch leads to fabrication of 1D PCs with mirror-like Si walls which is very desirable when using these structures as optical elements. The great advantage of these structures is the compatibility of their fabrication with current semiconductor processing techniques. This provides simplicity, accessibility and low cost during the fabrication of these PCs within optical integrated circuits<sup>7,8</sup>.

\*perovat@tcd.ie; phone 3 531 608-1432; fax 3 531 677-2442; <http://www.mee.tcd.ie>; Department of Electronic & Electrical Engineering, University of Dublin, Trinity College, Dublin 2, Ireland

Opto-Ireland 2005: Optoelectronics, Photonic Devices, and Optical Networks, edited by J. G. McInerney, G. Farrell, D. M. Denieffe, L. P. Barry, H. S. Gamble, P. J. Hughes, A. Moore, Proc. of SPIE Vol. 5825 (SPIE, Bellingham, WA, 2005) · 0277-786X/05/\$15 · doi: 10.1117/12.607252

Planar PCs, as well as vertically oriented multilayer coatings, possess various optical properties depending on the optical thickness ratio of their components. The optical thickness is the product of the refractive index and the geometrical thickness (width) of the layer,  $D$ , of the component within the structure. By selecting a material with a suitable value of  $n$  and the required values of  $D_i$  for different components within the structure, the reflection/transmission spectra of the corresponding PC can be simulated using, for example, the transfer matrix method<sup>9</sup>.

Let us consider, in detail, the type of information can be extracted from simulations prior to fabrication using grooved Si as a 1D PC<sup>6</sup>. The structure is fabricated by wet anisotropic etching forming grooves in the Si filled with air. The refractive index,  $n_{air}=1$ , and the thickness of these grooves,  $D_{air}$ , will be determined by the lattice constant of the regular structure  $A=D+D_{air}$ . The value  $A$  is normally very well controlled during the fabrication process and, so, by varying only one parameter,  $D$  or  $D_{air}$ , we can trace the change in the optical thickness of one component with respect to the other. This, in turn, will result in a change in the optical spectra allowing us to predict the photonic properties of these structures. In other words, if we want to fabricate a photonic crystal with particular properties, a systematic analysis of its photonic properties can be performed by choosing of the certain values of  $n$  and  $A$  and varying the value  $D$ , in order to obtain the dependence of the optical properties on the filling factor  $D/A$ . As a result of this procedure the so called gap map will be obtained<sup>1,10</sup>.

It should be noted that if one of the components has a high refractive index, like silicon in the infrared range with  $n_{Si}=3.42$ , then using air as the second component within the structure will generate a PC with a high optical contrast since  $n=n_{Si}/n_{air}=3.42$ . The advantages of building structures with high  $n$  are

- i) We can substantially reduce the number of structure periods,  $m$ ,
- ii) We obtain a wider PBG
- iii) The edge sharpness of the PBG is improved.

In addition, infiltration of the grooves with compounds having different  $n_i$  will change the optical thickness, resulting in structures with different photonic properties. For instance, if we fabricate a PC with empty grooves, we can easily alter the optical properties simply by filling the grooves with liquid crystals.

Hence, planar 1D PCs in comparison with vertical 1D PCs have three main advantages:

- i) The capability of moulding the light flow in a horizontal direction.
- ii) A high refractive contrast
- iii) The possibility of changing the optical characteristics by fabricating a composite PC structure.

In this study, we performed simulations of the optical properties of grooved Si structures and composite structures based on this material. We fabricated a number of these structures and probed their optical properties using an FTIR spectrometer in conjunction with an IR microscope. Finally, we compared the simulated properties to those measured experimentally.

## 2. CALCULATIONS OF THE OPTICAL CHARACTERISTICS

Reflection spectra for periodical structures of Si+Air, with refractive indices  $n_{Si}=3.42$  and  $n_{air}=1$  and thicknesses  $D_{Si}$  and  $D_{air}$ , were calculated using the transfer matrix method<sup>9</sup> for normal incidence of light from air as a surrounding medium. The optical matrix of the entire layered structure was then estimated using the following equation

$$S=[(I \cdot L)_{Si}(I \cdot L)_{air}]^m \cdot (I \cdot L)_{Si} \quad (1)$$

where  $(I \cdot L)_{Si}$  and  $(I \cdot L)_{air}$  are the optical matrixes of the Si and air layers respectively,  $m$  is the number of periods in the structure,  $I$  is the matrix of the interface between the layers and  $L$  is the matrix of the layer transmission.

The value  $I$  depends on the refractive indices of the components of the periodic structure, while the value of  $L$  depends on their thickness,  $D$ , and on the wavelength,  $\lambda$ . The reflectivity, or reflection coefficient,  $R$  was calculated from the following equation

$$R(\lambda) = | [S(\lambda)I, 0 / S(\lambda)0, 0]^2 | \quad (2)$$

The band gap regions were calculated as follows<sup>10</sup>. First, reflection spectra for values of  $D_{Si}/A$  ranging from 0.01 to 0.99 were calculated for the optimal lattice period value,  $m=6$  (see Fig. 1a). From the reflection spectrum, obtained for each  $D_{Si}/A$ , the values of  $A/\lambda$  corresponding to the edges of the bands with  $R>0.99$  were extracted and plotted versus  $D_{Si}/A$  as shown in Fig. 1b. The series of closed regions obtained represents the so-called gap map of PBGs<sup>1</sup>.

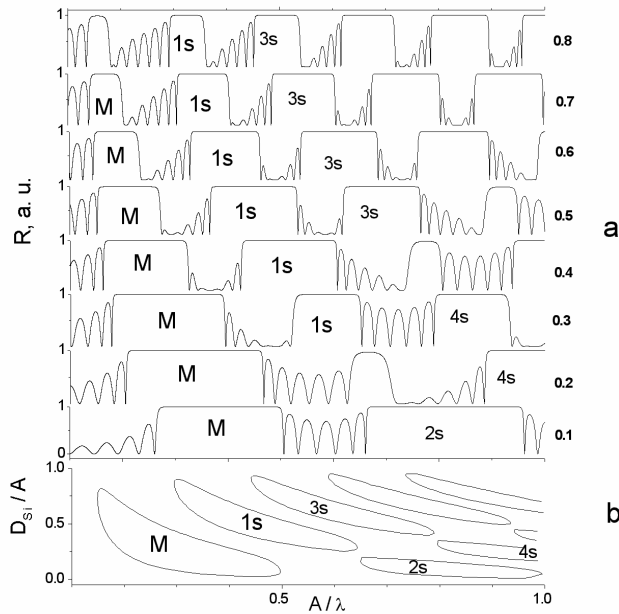


Figure 1:  
a) Calculated reflection spectra of 1D PC (Si+Air) versus the filling factor  $D_{Si}/A$  (corresponding values shown beside each spectrum).  
b) The gap map for the main (M) and nearest secondary (1s-4s) band gaps

The largest area in the figure, shown in Fig. 1b in the range  $A/\lambda = 0.15-0.5$ , represents the main band gap, since its band gaps are located in the range of lower frequencies for the majority of values of  $D_{Si}/A$ . The smaller closed figures, which represent secondary band gaps, are also seen in a range of  $A/\lambda$  from 0.3 to 1.0 and above. For values of  $D_{Si}/A$  higher than 0.8 some secondary band gaps appear in the low-frequency range.

Using this gap map we can obtain the point of intersection of certain bandgap regions by choosing some particular value of  $D_{Si}/A$  and drawing a horizontal line on the plot through this value. The X coordinates corresponding to these points allow us to determine the regions of PBGs, in unitless coordinates  $A/\lambda$ , for a particular  $D_{Si}/A$  of the periodic structure.

For example, the main photonic band gap can be used for obtaining a structure with PBG in the region of  $A/\lambda = 0.15-0.5$ . However, by taking the secondary band gaps into account the PBG can be even extended to  $A/\lambda = 1$  and beyond. Moreover, it was found that the secondary band gaps for values of  $D_{Si}/A = 0.4-0.9$  can be even wider in frequency than the main PBG. Therefore, the PBGs gap-map shown in Fig. 1b, which describes the optical characteristics of the periodic structure with respect to its geometrical parameters (filling factor), allows the design of optical devices for user specified regions to be performed.

The presence of PBGs in certain spectral region is not the only factor to be considered during the design of the photonic crystal. From an application point of view, it is important to have a band gap with sharp edges, that is with high maximum values of  $R$  combined with small minimum values of  $R$ . In addition, the transition from the high  $R$  region to the low  $R$  region should occur within a short interval of wavelength. As can be seen from Fig. 1a, the spectra with  $D_{Si}/A = 0.3$  (band 1s),  $D_{Si}/A = 0.5-0.7$  (the main band gap M) and  $D_{Si}/A = 0.6-0.8$  (band 1s) satisfy these criteria. Therefore, in order to obtain sharp edges on the main and secondary bands in the reflection spectra the filling factor must be chosen carefully. Note that the numbering of the secondary PBGs is relative.

If the optical or geometrical parameters of one of the components in the periodic structure is changed we alter the optical characteristics of the structure<sup>11</sup>. One of the easiest ways to achieve such a change is to fill the grooves with liquid crystals. In accordance with<sup>12</sup> the refractive index of the nematic liquid crystal E7 in the mid-infrared range is  $n_r = 1.54$

in the isotropic phase at a temperature of 62<sup>0</sup>C. In the nematic phase at room temperature at 23<sup>0</sup>C E7 has two values of refractive index in IR range <sup>13</sup>, viz: ordinary,  $n_o=1.49$  and extraordinary,  $n_e=1.69$  due to the alignment of the long molecular axis of the LC. This provides us with an opportunity to tune the properties of the composite structure by using temperature, thermo-tuning, or an applied electric field, electro-tuning. In the first case the refractive index of the LC is changed due to a phase transition caused by the change in temperature heating while in the second case the alignment of the LC molecules is changed by the applied electric field. These changes in refractive index are clearly illustrated by the schematic showing the various LC orientations possible within grooves, shown in Fig. 2.

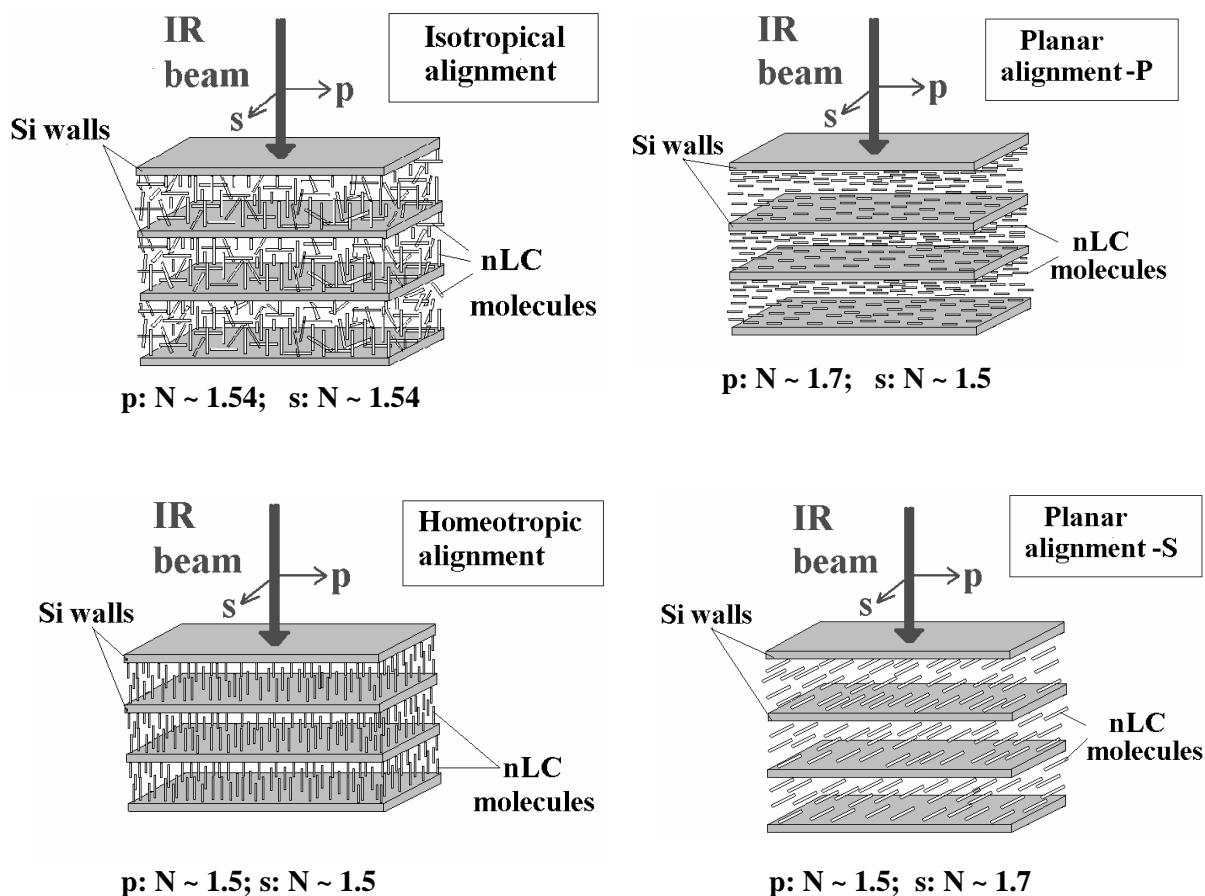


Figure 2: Schematic of different types of nematic LC alignment with the corresponding values of the refractive indexes along S and P directions.

We now consider the influence of the value of the refractive index on the optical properties of photonic composites. Fig. 3 shows the PBGs gap map for a grooved Si photonic crystal before and after its infiltration with E7 ( $n_{LC}=1.54$ ). The refractive index contrast for these two structures is  $3.42/1=3.42$  and  $3.42/1.54=2.22$ , respectively. From the gap map for the composite structure consisting of Si + LC, the main as well as the secondary PBGs are approximately halved in area and shifted to the higher wavelength (red shift) in comparison with the gap map for the Si+air structure. Therefore, building a Si+air structure with a certain  $D_{Si}/A$ , we can redesign the optical spectrum of the PC simply by filling the air space with compounds with a variety of refractive indices, liquid crystals in our case. This ability is particularly important if other values of  $D_{Si}/A$  cannot be used for the Si + Air PC.

The gap maps for the composite structure were calculated and plotted taking into account the largest possible changes in the refractive index of the LC in the grooves, viz. 1.49 and 1.69. For practical applications only the main and the closest secondary band gap will be useful, therefore only the PBGs for the main and the three closest secondary band

gaps are shown in Fig. 4. As can be seen from this figure, the variation in the refractive index results in a shift of the short-wave edge of the band only, that is, a shift to higher wavelengths with an increase of  $n_{LC}$  for the main PBG (M) and for the secondary PBG (2s). In the lower secondary PBGs (1s and 3s) a red shift of both PBGs edges is observed. The shift of the edge can be as large as  $A/\lambda = 0.04$  for the main PBG ( $D_{Si}/A=0.133$ ) and  $A/\lambda = 0.08$  for the secondary PBG ( $D_{Si}/A=0.07$ ). To summarise, an analysis of the photonic band gap allows us to define the optimal parameters for the design and fabrication of 1D photonic crystals based on Si.

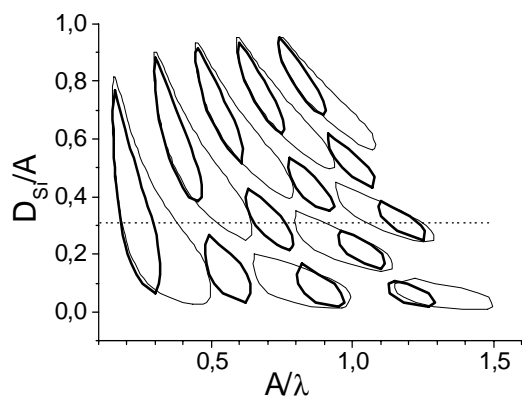


Figure 3: The gap map of PBGs (with reflection  $R > 0.99$ ) for photonic structures Si+Air (thin line) and Si+LC (thick line) with number of periods  $m=6$ ,  $n_{Si} = 3.42$ ,  $n_{LC} = 1.54$  (isotropic phase) and normal incidence of light.

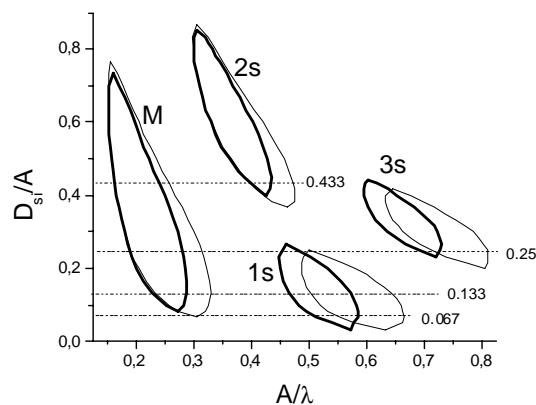


Figure 4: The gap map for a composite PC infiltrated with LC shown for the main (M) and for the three nearest photonic band gaps (1s-3s), calculated for two values of refractive indexes  $n_{LC} = 1.49$  (thin line) and  $1.69$  (thick line). The dashed lines corresponding to the certain values of  $D_{Si}/A$  intersect the band gap regions with maximum shift of their edges.

### 3. EXPERIMENTAL

#### 3.1 Fabrication of 1D PCs

1D PCs with lattice constants  $A=2, 3$  and  $4 \mu\text{m}$ , with fixed filling factors  $D_{Si}/A$  and a number of periods  $m=6$  were obtained by wet anisotropic etching of grooves in (110) oriented Si. The details of this procedure were described elsewhere<sup>14</sup>. In order to obtain a composite photonic crystal, Si+LC, the nematic liquid crystal E7<sup>12</sup> was infiltrated into the grooves. Control of the infiltration process was monitored using an optical microscope with a magnification of 500x.

#### 3.2 FTIR measurements

Infrared reflection and transmission spectra were measured with an FTS 6000 FTIR spectrometer in conjunction with a UMA 500 infrared microscope in the wavelength region  $\lambda=1.4-15 \mu\text{m}$  under normal incidence of light. During the experiment the incidence of the infrared light beam on the structure was as shown on the left in Fig. 5 and described elsewhere in detail<sup>15</sup>. A schematic of the birefringence measurements is shown on the right in Fig. 5, see also Ref.<sup>16</sup> for details. The electric vector  $E$  of the incident light was oriented either parallel or perpendicular to the grooves, corresponding to the propagation, in an artificial crystal, of ordinary ( $o$ ) or extraordinary ( $e$ ) rays, respectively.

## 4. RESULTS AND DISCUSSIONS

### 4.1 Photonic properties of 1D PCs

Infrared spectra were measured for photonic crystals before and after infiltrating the structure with a liquid crystal. A simulation of the spectrum  $R$  was carried out using Eqns. (1) and (2) and  $D_{Si}/A$  as a free parameter until the best agreement between the experimental and theoretical spectra was achieved for the uninfiltreated crystal. This procedure was necessary in order to obtain an accurate determination of the structural parameters of the photonic crystal,  $D_{Si}$  and  $D_{air}$ , which were initially estimated from SEM measurements. These parameters could deviate from those measured due to slight etching of the Si walls occurring during the fabrication process. Next, keeping the geometrical parameters obtained constant, simulations of the spectrum for the composite PC were performed while varying the value of  $n_{LC}$ .

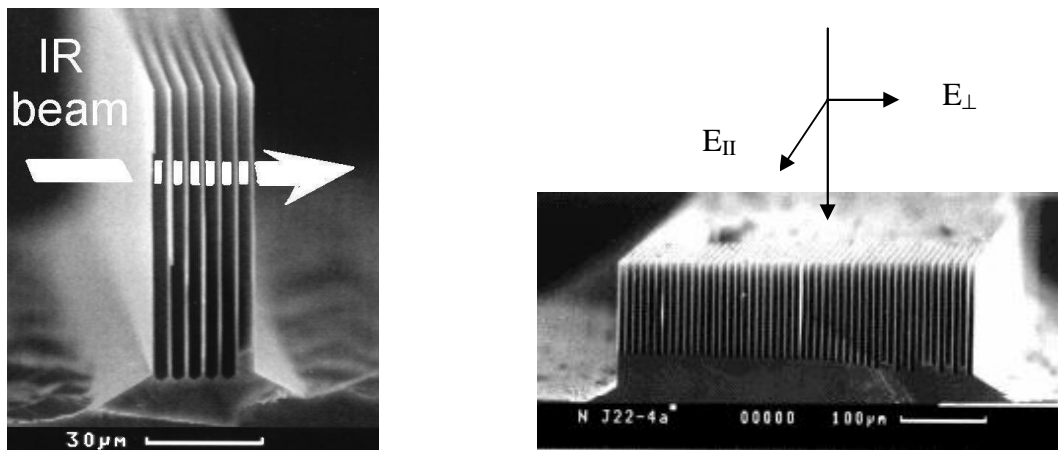


Figure 5: 1D PC samples for photonic (left) anisotropic (right) measurements.

The experimentally obtained spectra for empty sample with  $A=3 \mu\text{m}$  are presented in Fig. 6b. They show the existence of wide PBGs in both the reflection and transmission spectra. Fig. 4 also shows good agreement between maxima in the spectrum of  $R$  and minima in the spectrum of  $T$ . The high values of transmission indicate that light losses in these structures are minimal. This structure possesses secondary PBGs with  $R=80\%$ , in, for example, the region  $\lambda=5-7 \mu\text{m}$ , as well as large signal modulation of  $\sim 60\%$ , calculated as the difference between the maxima and minima in the spectrum  $R$ , which is very important for application in optical integrated circuits.

The calculated spectrum of the PC structure with  $D_{Si}/A=0.4$  and a main PBG in the region  $9.7-17.7 \mu\text{m}$  is presented in Fig. 6c, while the PBGs gap map for all possible structures with  $A=3 \mu\text{m}$  is shown in Fig. 6a. Only part of the main PBG is seen from the experimental spectra in Fig. 6b for a PC with  $A=3 \mu\text{m}$ . This is because the long wavelength range is limited due to the cut off for the IR microscope MCT detector at  $14.5 \mu\text{m}$ , whilst the main PBG in accordance with Fig. 6a, extends to higher wavelengths. The reduction of parameter  $A$  down to  $2 \mu\text{m}$  leads to a shift of the main PBG to shorter wavelengths (blue shift). We can observe the whole main PBG in the PC with reduced  $A$ , since this new structure has a main PBG in the region  $6.5-12 \mu\text{m}$ , which can be measured with our MCT detector. This is shown in Fig. 7b. The calculated spectrum  $R$  for this structure is shown in Fig. 7c, from which the wide secondary band gap is also seen in the region of  $3-5 \mu\text{m}$ . It is worth noted that the relatively wide secondary band gaps are characteristic of PCs with a high refractive index contrast. This fact allows us to use the same photonic structure in the shorter wavelength range without decreasing the lattice constant.

As can be seen from Fig. 7a, infiltration of the LC E7, with a refractive index  $n \approx 1.6$ , into the grooves instead of air results in a reduction of the PBG's width for both the main and the secondary band gaps and leads to their red shift. The thick line for experimental and calculated spectra shown Fig. 7b and 7c demonstrates this effect clearly. From Figs. 7 b

and 7c a good agreement between the experimental and calculated spectra for both the original PC and the composite PC (Si+LC) is observed.

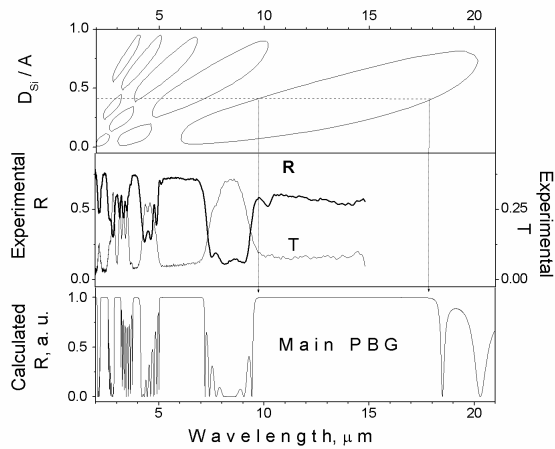


Figure 6: a) PBG regions (with  $R > 0.99$ ) for 1D PC “Si+Air” with number of periods  $m=6$ , lattice period  $A=3 \mu m$  calculated at normal incidence of light; b) experimental reflection  $R$  and transmission  $T$  spectra; c) simulated reflection spectrum obtained by best fit to the experimental spectrum for  $D_{Si}=1.2\mu m$  ( $D_{Si}/A = 0.4$ ).

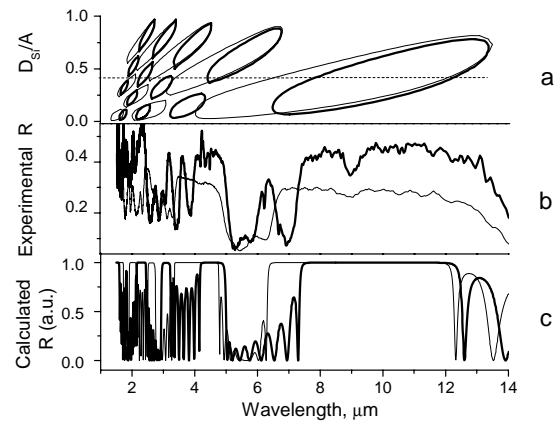


Figure 7: PBG regions ( $R > 0.99$ ) of empty (thin line) and LC E7 infiltrated (thick line) 1D PC shown as a) gap map, b) experimental reflection spectra and c) calculated spectra for  $D_{Si}/A=0.4$ . The structure parameters are:  $m=6$  and  $A=2 \mu m$ .

As was already mentioned in Section 2 the long molecular axis of LC molecules in the mesophase can be aligned in one direction. If the electric field of the incident light is suitably oriented these materials can possess their anisotropic optical properties. We have estimated the maximal effect produced by electro-tuning and thermo-tuning on optical properties of 1D PC composite. For this purpose the structure with  $D_{Si}/A=0.133$  has been chosen from the gap map shown in Fig. 4, because this structure possess the largest shift of PBGs after LC infiltration. The calculated spectra for demonstrating the electro-tuning effect under the change of the refractive index from  $n_o$  to  $n_e$  are shown in Fig. 8 c. The shift of the low-wavelength edge of the main PBG observed in this case is estimated to be  $\Delta\lambda/\lambda \approx 10\%$  (here  $\lambda$  corresponds to the centre of PBG). The thermo-tuning effect on the shift of the low-wavelength edge of the main PBG for different refractive indices ( $n_o$  to  $n_e$ ) in nematic phase is shown in Figs. 8 a and b. We can see that the effect is smaller in this case and can be estimated to be  $\sim 5\%$  in average and  $\sim 7\%$  for the largest difference in the refractive indices (see Fig. 8 b).

Fig. 9b shows the experimentally obtained reflection spectra for a composite PC with  $A=4 \mu m$ . The width of the Si walls was determined as a result of the spectra fitting procedure outlined earlier and gave values of  $D_{Si}=2.3 \pm 0.05 \mu m$  (or  $D_{Si}/A=0.58$ ). The intersection of a line drawn from this point with the PBG map for the original matrix gives the position of the main band gap in the region  $\lambda=17-26 \mu m$  (not shown in Fig.9). However, the secondary band gap, shown in Fig. 9 has a band gap ranging from  $\lambda=8.7$  to  $11.7 \mu m$ . After infiltration of the original photonic crystal with E7 in accordance with the gap map we should expect the red shift of this secondary band gap. This is confirmed by the experimental spectrum shown in Fig. 9b. Moreover, the shift between the edges of the bands,  $\Delta\lambda=0.4 \mu m$ , for  $E_{||}$  and  $E_{\perp}$  spectra is also seen from Fig. 9b. This shift suggests the presence of anisotropic layers in the PC, resulting from the LC alignment.

Note that the spectrum  $E_{||}$  corresponds to the orientation of the electric vector of the reflected light along the grooves, whilst spectrum  $E_{\perp}$  corresponds to the orientation of the electric vector perpendicular to this direction. Therefore, from spectra obtained at different polarizations of the incident light, we extracted information on the LC alignment, obtained as a result of the liquid crystal flow during the infiltration process. The  $\lambda$  positions for the PBG edges of  $E_{||}$  and  $E_{\perp}$  spectra are in a good agreement with the gap map and with the simulated spectra shown in Fig. 9c. The values of  $n_{LC} = 1.52$  and  $1.67 (\pm 0.02)$  for  $E_{||}$ - and  $E_{\perp}$ -polarisations, respectively, have been estimated from the fitting procedure. An

anisotropy value for the LC layers ( $\Delta n_{LC} = 0.15$ ) is relatively close to the known value for  $\Delta n_{LC}$ , which is equal to  $n_e - n_o = 1.69 - 1.49 = 0.2$ <sup>13,17</sup>. In fact, the deviation obtained shows that the alignment of E7 LC in studied composite structure is not perfect. These results show the possibility of using this particular type of 1D PC as a polarized filter in optical integrated circuits.

Based on the results of simulation for the structure shown in Fig. 9 we conclude that the directors, or long molecular axes, of the E7 LC are aligned along the Si walls in a planar alignment. It should be noted that if the initial alignment of LC molecules is planar then, after a voltage is applied between the Si walls, this alignment will change to a homeotropic one, with the long molecular axes aligned along the direction of the electric field. Therefore, the initial planar alignment is very important for obtaining the maximum electro-tuning effect for composite structures infiltrated by liquid crystals with positive anisotropy.

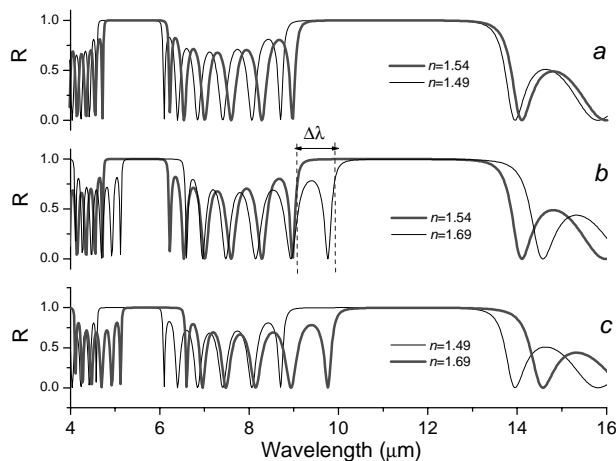


Figure 8: The comparison of calculated PBG regions ( $R > 0.99$ ) of 1D PC+LC composite structure shown as a result of a) and b) thermo-tuning effect and c) electro-tuning effect. The structure parameters used for calculations are:  $D_{Si}/A = 0.133$ ,  $m = 6$  and  $A = 3 \mu\text{m}$ .

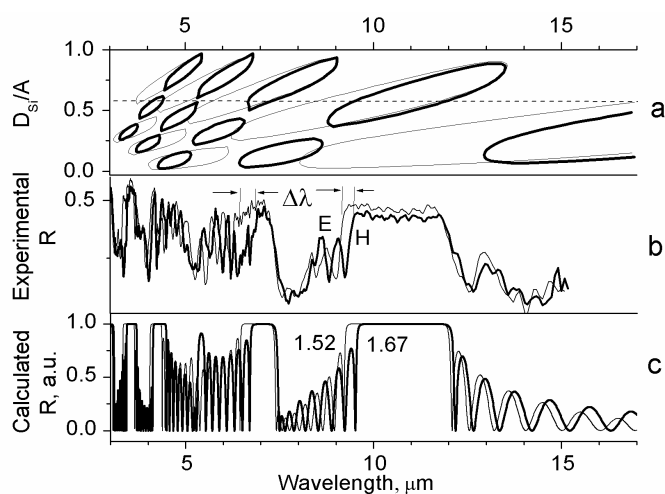


Figure 9: PBG regions of empty and LC infiltrated 1D PC with period  $A = 4 \mu\text{m}$  and  $m = 6$ : (a) gap map of empty PC matrix (thin line) and PC+LC composite (thick line), (b) experimental spectra of infiltrated sample for  $E_{||}$  (thin line) and  $E_{\perp}$  (thick line) polarized light, (c) spectra of PC+LC composite with  $D_{Si}/A = 0.58$  calculated for the refractive indices of 1.52 (thin line) and 1.67 (thick line).

#### 4.2 Optical anisotropy of grooved Si

The fabricated structures possess not only photonic properties, that is, the existence and tuning of PBGs, but also have strong anisotropic properties. A schematic of the birefringence measurements is shown on the right of Fig. 5. Infrared spectra obtained at different polarization  $E_{||}$  and  $E_{\perp}$  during these measurements for the sample with  $A = 6$  and  $m = 50$  are shown in Fig. 10. The spectra demonstrates beats in the short-wavelength range, which disappear on passing to the range where the radiation wavelength exceeds the lattice constant of the artificial crystal,  $\lambda > A$ . It can be seen that the spectra

recorded at different polarizations differ dramatically: the reflection at  $E_{\parallel}$  is much stronger than at  $E_{\perp}$ . We can conclude, therefore, that the refractive index for an ordinary ray is much higher than for an extraordinary one,  $n_o > n_e$ , i.e. grooved Si is an effective medium in the form of a negative uniaxial crystal whose axis is perpendicular to the silicon walls. The birefringence value  $\Delta n \approx 1.3$  found for this material [16] is much larger than any known value for existing natural birefringent materials. This allows to use these structures as a reflecting polarizers for the infrared range.

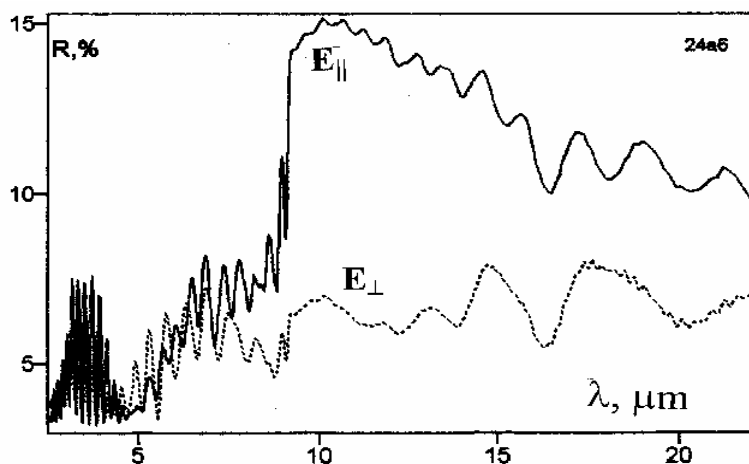


Figure 10: Reflection spectra of grooved Si anisotropic structure measured at two polarisations of light  $E_{\parallel}$  and  $E_{\perp}$ .

## 5. CONCLUSION

Periodically grooved Si structures with different lattice constants ranging from 2 to 6  $\mu\text{m}$  and a variety of lattice periods were designed and fabricated. It has been shown that the simulation of the optical characteristics for these structures can be performed by using the characteristic matrix method. The gap maps were also obtained from the spectra simulation, which allows the design of optical devices for user specified regions to be performed. These devices, acting as 1D photonic crystal can be used from near to far infrared range and are promising candidates for application in Si based monolithic photonics. Infiltrating the grooves with liquid crystals results in the formation of composite photonic crystals and will allow tuning of their optical properties. A shift of the PBG's edges by a factor  $\Delta\lambda/\lambda \approx 7\%$  was predicted as a result of a thermo-tuning effect and  $\sim 10\%$  as a results of electro-tuning effect.

## ACKNOWLEDGMENTS

The authors would like to thank A. Nashchekin for SEM images of the samples under study. The work was supported partly by Science Foundation Ireland (Grant 04/BR/P0698) and partly by funds from the Programmes "Optics and Laser Physics".

## REFERENCES

1. J. D. Joannopoulos, R. D. Meade, and J. N. Winn, *Photonic Crystals: Molding the Flow of Light*, Princeton University Press, Singapore, 1995.
2. E. Yablonovitch, "Inhibited Spontaneous Emission in Solid-State Physics and Electronics", *Phys. Rev. Lett.* **58**, pp.2059-2062, 1987.
3. J.S. Foresi, P.R. Villeneuve, J. Ferrera, E.R. Thoen, G. Steinmeyer, S. Fan, J.D. Joannopoulos, L.C. Kimerling, H.I. Smith, and E.P. Ippen, "Photonic-bandgap microcavities in optical waveguides", *Nature*, **390**, pp.143-145, 1997.
4. C. A. Barrios, V. R. Almeida, P. Panepucci and M. Lipson, "Electrooptic Modulation of Silicon-on-Insulator Submicrometer-Size Waveguide Devices", *Journal of Lightwave Technology* **21**, pp. 2332-2339, 2003.
5. S.-S. Yun and J.-H. Lee, *J.Micromech. Microeng.*, **13**, 721, 2003.
6. V. Tolmachev, E. Astrova, T. Perova, "1D photonic crystals based on periodically grooved Si", *Proceedings SPIE*, **5401**, pp.192-199, 2004.
7. K. Busch, S. Lölkes, R. Wehrspohn, H. Föll (eds.) *Photonic Crystals. Advances in Design, Fabrication, and Characterization*, Wiley-VCH, Germany, p.420, 2004.
8. M. Lipson, "Switching light on a silicon chip", *Opt.Mater.*, **27**, pp.731-739 (2005).
9. R.M.A. Azzam, N.M. Bashara, *Ellipsometry and polarized light*, North-Holland. Amsterdam, Netherlands, (1977); M. Born and E. Wolf, *Principles of Optics, 4<sup>th</sup> edition*, Pergamon, Oxford, (1969).
10. V.A. Tolmachev, T.S. Perova and K. Berwick, "Design criteria and optical characteristics of 1D photonic crystals based on periodically grooved silicon", *Appl. Opt.* **42**, p.5679, 2003; V.A. Tolmachev, Reflectance spectra and photonic band gaps of a one-dimensional photonic crystal based on a silicon-air periodic structure, *Rus. Opt.&Spectr.*, **97**, pp.276-279, 2004.
11. K. Busch, and S. John, "Liquid-crystal photonic-band-gap materials: the tunable electromagnetic vacuum", *Phys. Rev.Lett.* **83**, pp.967-970, 1999.
12. I.C. Khoo, "The Infrared Optical Nonlinearities of Nematic Liquid Crystals and Novel Two-wave Mixing Processes", *J. Mod. Opt.*, **37**, p.1801 (1990).
13. Data Sheet Licristal® E7, Merck KGaA, Germany, 2001.
14. V.A. Tolmachev, L.S. Granitsyna, E.N. Vlasova, B.Z. Volchek, A.V. Nashchekin, A.D. Pemenyuk and E.V. Astrova, "1D-photonic crystal obtained by vertical anisotropic etching of silicon", *Semiconductors*, **36**, pp. 932-937 (2002).
15. V.A. Tolmachev, T.S. Perova, E.V. Astrova, B.Z. Volchek, and J.K. Vij, "Vertically etched silicon as 1D photonic crystal", *Physica status solidi (a)*, **197**, pp.544-549, 2003.
16. E.B.Astrova, T.S.Perova, V.A. Tolmachev, A.D. Pemenyuk, J.Vij and A.Moore, "IR Birefringence in Artificial Crystal Fabricated by Anisotropic Etching of Silicon", *Semiconductors*, **37**, pp.417-421, 2003.
17. S.-T. Wu, "Infrared properties of nematic liquid crystals: an overview", *Opt. Eng.*, **26**, pp. 120-128, 1987.